Biophysical Journal, Volume *122*

Supplemental information

Surface viscosities of lipid bilayers determined from equilibrium molecular dynamics simulations

James E. Fitzgerald III, Richard M. Venable, Richard W. Pastor, and Edward R. Lyman

S 1 MINIMIZATION AND EQUILIBRATION PARAMETERS FOR THE STANDARD LENNARD-JONES POTENTIAL CUTOFF SIMULATIONS

Step	Integrator	Position Strength	Dihedral Strength	P Coupling	T Coupling	dt (fs)	N Steps
Minim.	Steepest Descent	1000	1000	None	None	N/A	5000
Equil. 1	MD	1000	1000	None	Berendsen (1)	1	125000
Equil. 2	MD	400	400	None	Berendsen	1	125000
Equil. 3	MD	400	200	Berendsen	Berendsen	1	125000
Equil. 4	MD	200	200	Berendsen	Berendsen	2	250000
Equil. 5	MD	40	100	Berendsen	Berendsen	2	250000
Equil. 6	MD	None	None	Berendsen	Berendsen	2	250000

Table S1: 'Position Strength' refers to the strength of the position restraints, constraining the Phosphorous atoms in the lipid headgroups to the xy-plane ($\mathrm{kJ/(mol\,nm^2)}$). 'Dihedral Strength' refers to the strength of the dihedral restraints, restricting the shapes of the branch in the lipid backbones, as well as any double bonds in the hydrocarbon chains ($\mathrm{kJ/(mol\,rad^2)}$).

S 2 PARAMETERS FOR SIMULATIONS COMPARING STANDARD AND LONG-RANGE CUTOFFS

Lipid	van der Waals	t_{run}	A (Å^2)	Cell c (Å)	L (Å)	$h_w/2$ (Å)
DPPC	VFSWITCH	400	63.0	68.09	95.25	13.29
DPPC	LJ-PME	400	62.6	67.16	94.94	13.06
DOPC	VFSWITCH	500	69.4	66.26	99.99	12.58
DOPC	LJ-PME	500	69.2	65.11	99.83	12.23

Table S2: Details of the NVT 288 lipid simulation systems used to compute the surface viscosity and lipid diffusion: t_{run} is post equilibration analytical interval; A is surface area/lipid; c is cell height along bilayer normal; L is bilayer edge length; $h_w = H - h$ is the total water thickness (see Figure 1) and $h_w/2$ is used to estimate D^{∞} from the Periodic Saffman-Delbruck model. DPPC and DOPC systems contained 30.4 and 33.5 waters/lipid, respectively.

T °C	Volume	Viscosity	Experiment
20	78.237	0.341(3)	1.002
25	78.554	0.322(1)	0.890
30	78.894	0.311(3)	0.798
40	79.594	0.278(2)	0.653
50	80.341	0.256(3)	0.547

Table S3: LJ-PME simulation viscosity (mPa s) and volume (nm^3) of TIP3P water at five temperatures. For viscosity, the standard error in the final digit is given in parentheses. Experimental values of water are listed in the last column.

S 3 ALL AUTOCORRELATION INTEGRALS

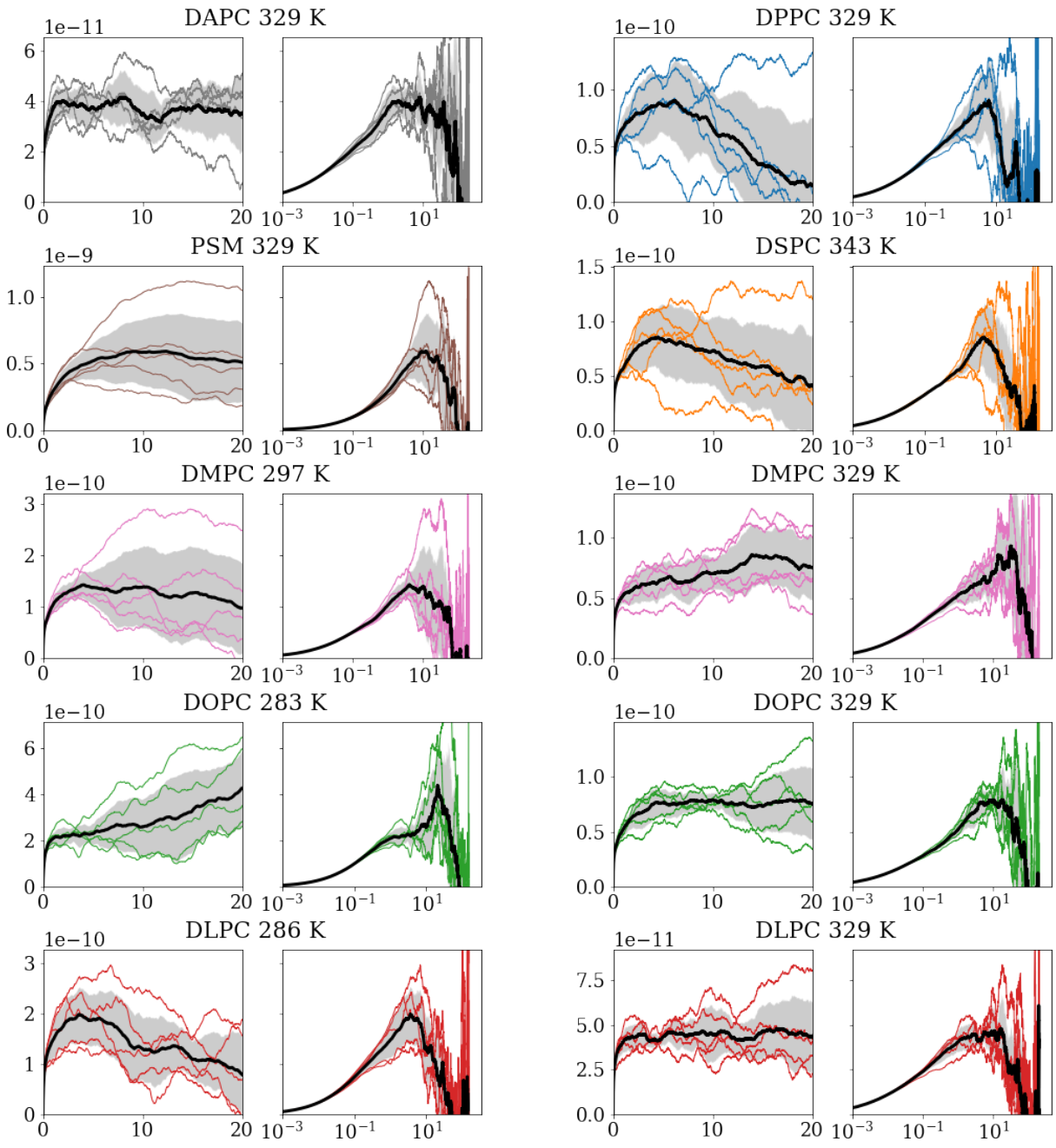

Figure S1: Autocorrelation integrals for all systems at all temperatures. Colored curves are the individual simulations. Solid heavy line is the average of those five, with standard deviation of the five replicas in gray. Continued in Figure S2. Autocorrelation integrals in Pa m s, and times in ns. Pairs of adjacent plots show the same data, on linear and logarithmic time-scales.

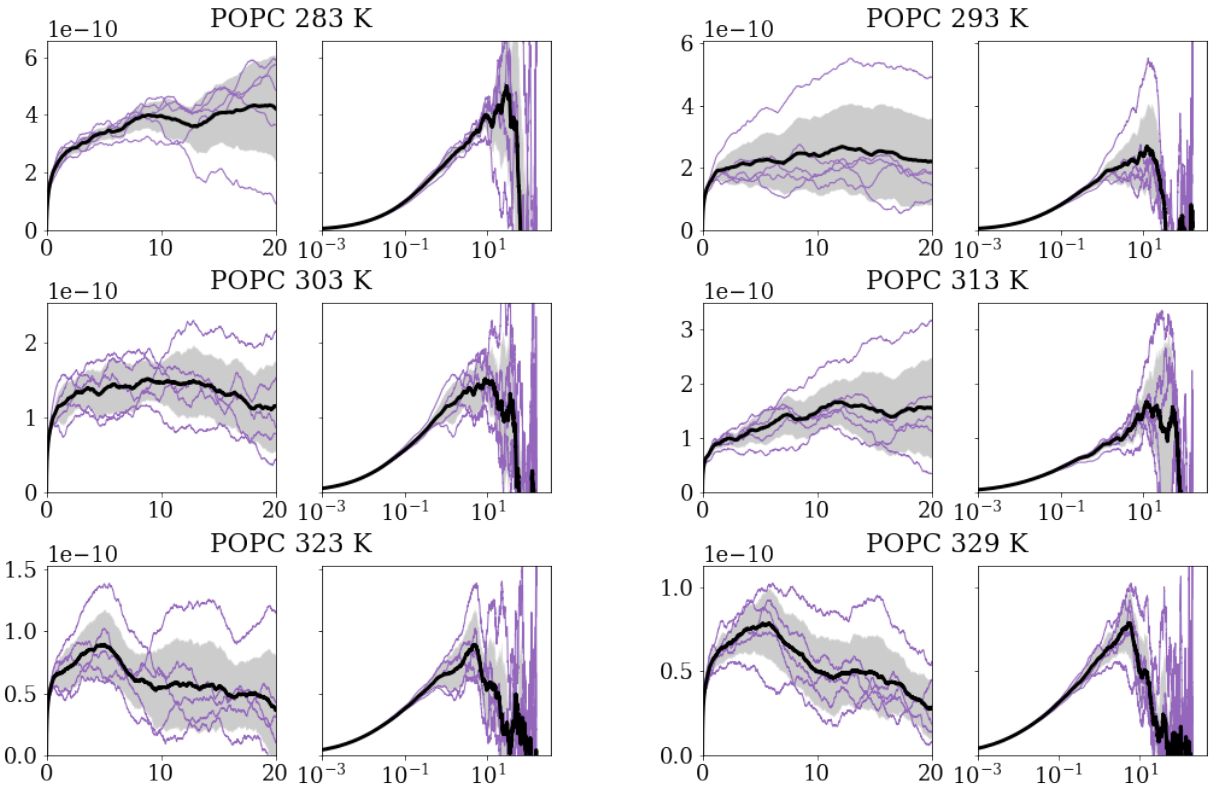

Figure S2: Autocorrelation integrals continued.

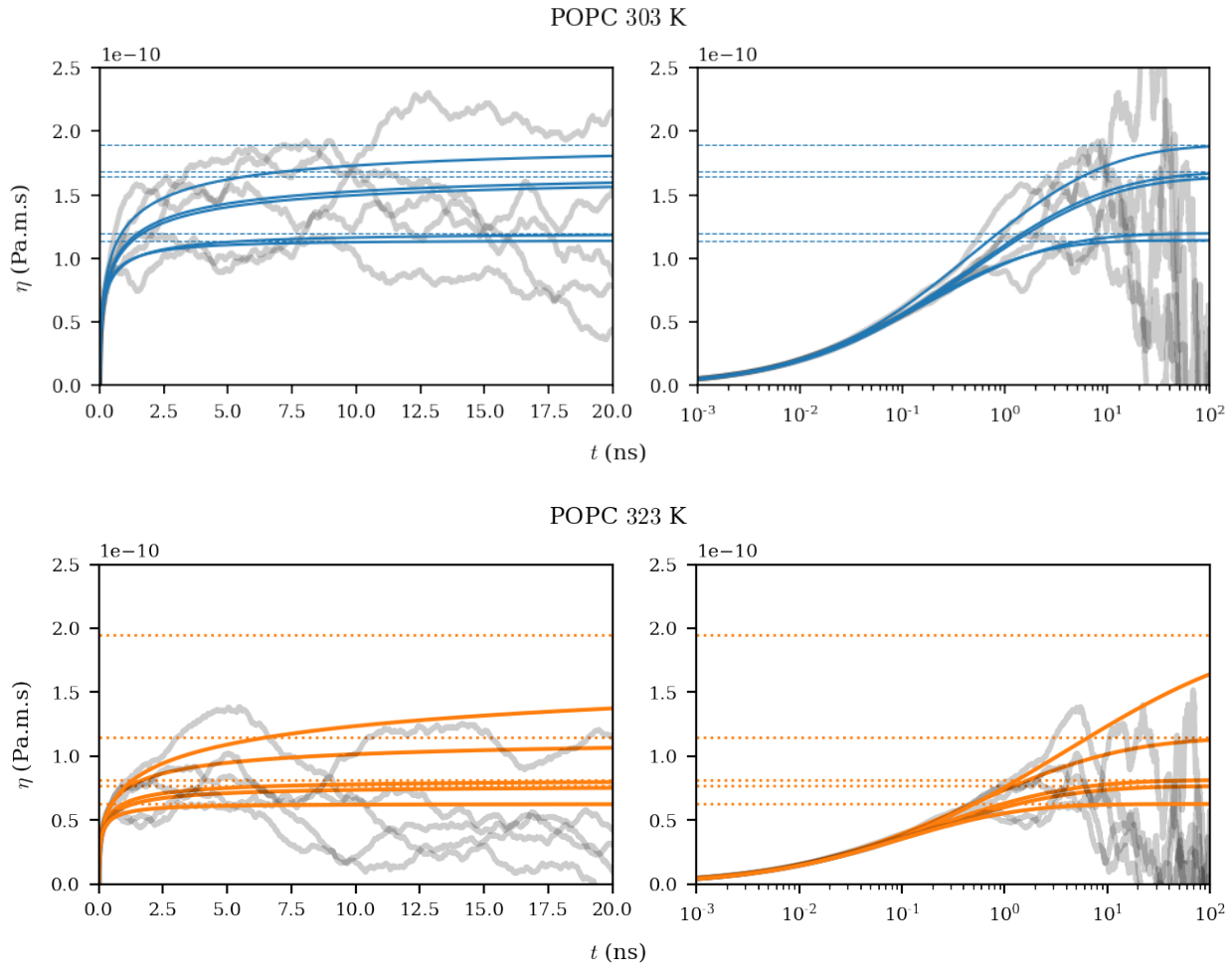

Figure S3: Lower incomplete gamma function fits to two sets of replicas for POPC at low- and high-temperature. Measured autocorrelation integral in gray, fits in solid color, and asymptotes in thin dotted colored lines. Note the tendency of the data to apparently undershoot the fit asymptotes. As in Figure S1, pairs of adjacent plots show identical data and fits, on linear and logarithmic time scales.

S 4 TIP3P VISCOSITY AT ARBITRARY TEMPERATURE

TIP3P viscosity data for a selection of temperatures was obtained from (2). In order to apply this viscosity data to temperatures not explicitly measured in (2), this was fit to a VFT model (3) as in Eq. 15, with great success. TIP3P viscosities at different temperatures were interpolated using this fit. Results of this fit are shown in Figure S4.

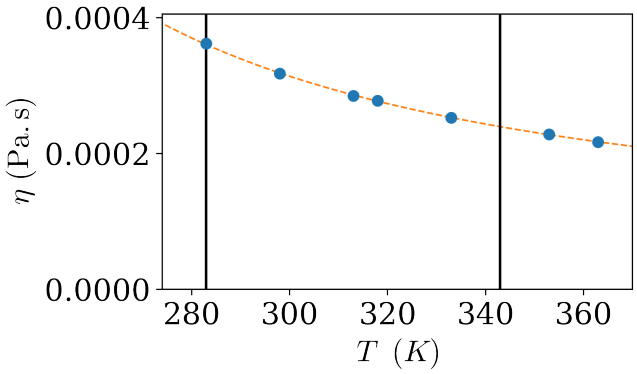

Figure S4: Fit of TIP3P viscosity data from (2). Errorbars are present but smaller than the datapoints. Orange shows the fit to Eq. 15. Black vertical lines show the highest and lowest temperatures used in the present work.

S 5 STRETCHED EXPONENTIAL FIT

The viscosity autocorrelation integral was fit to three assumed forms:

$$\eta(t) \approx a \int_0^t e^{-t'/\tau} \mathrm{d}t' \qquad = a\,\tau \left(1 - e^{-t/\tau}\right) \tag{1}$$

$$\eta(t) \approx a \int_0^t c\, e^{-t'/\tau_1} + (1-c) e^{-t'/\tau_2} \mathrm{d}t' \qquad = a \left[c\tau_1 \left(1 - e^{-t/\tau_1}\right) + (1-c)\tau_2 \left(1 - e^{-t/\tau_2}\right)\right] \tag{2}$$

$$\eta(t) \approx a \int_0^t \exp\left[-\left(\frac{t'}{\tau}\right)^{1/b}\right] \mathrm{d}t' \qquad = a\, b\, t_0 \gamma\left[b, \left(\frac{t}{t_0}\right)^{1/b}\right] \tag{3}$$

and the results of these fits are shown in Figure S5. The autocorrelation integral for each replica was fit to a lower incomplete gamma function, using the integrals from 10 ps–3.5 ns. At lagtimes below 10 ps, the autocorrelation function is highly oscillatory, so we excluded this portion from the fit. The fits were weighted using the inverse variance of the five replicas' integrals at each timestep. We also found better performace by using logarithmically subsampled points within that interval.

This fit was performed using the basin-hopping algorithm (4). As a rigorous test of the robustness of this algorithm, the data was fit over a wide range of initial values of the stretching exponent values b, using both least-squares and basin-hopping. The results of this are shown in Figure S6. The basinhopping fits give consistent results regardless of initial guess of parameters. This is extremely important in a fitting algorithm, as the 'true' parameter values are not known beforehand—especially in a complicated form such as this stretched exponential.

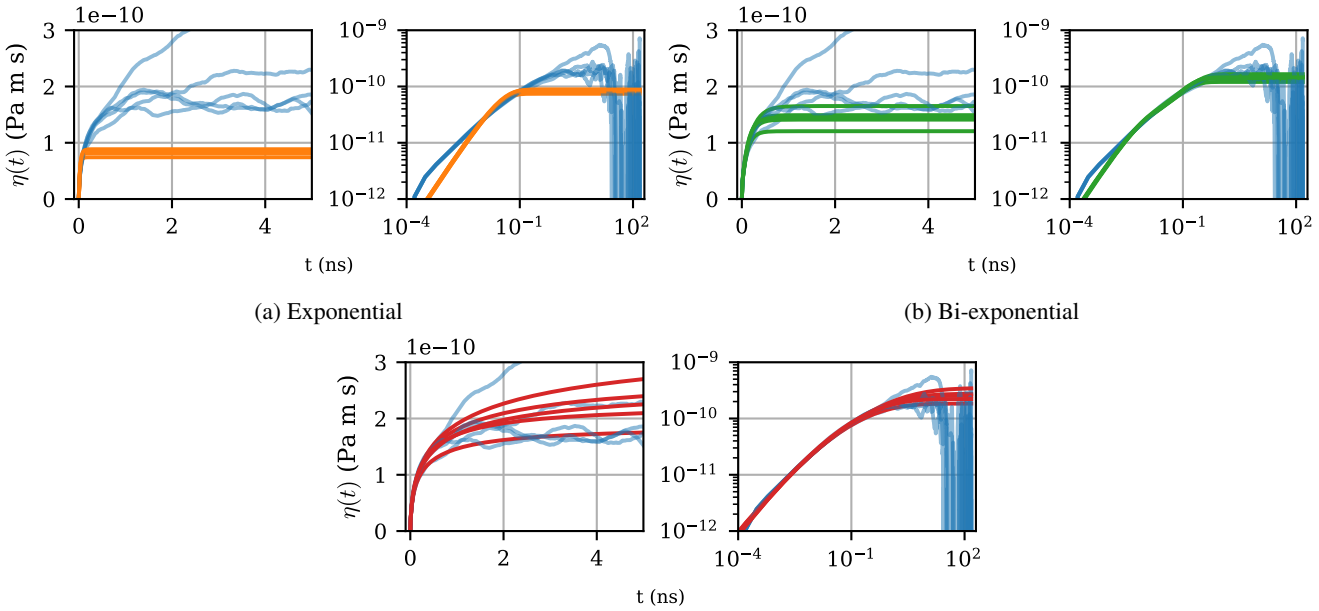

(a) Exponential

(b) Bi-exponential

(c) Stretched Exponential

Figure S5: The autocorrelation integrals for all 5 replicas of POPC at 293 K with (a) exponential, (b) bi-exponential, and (c) stretched exponential integral fits.

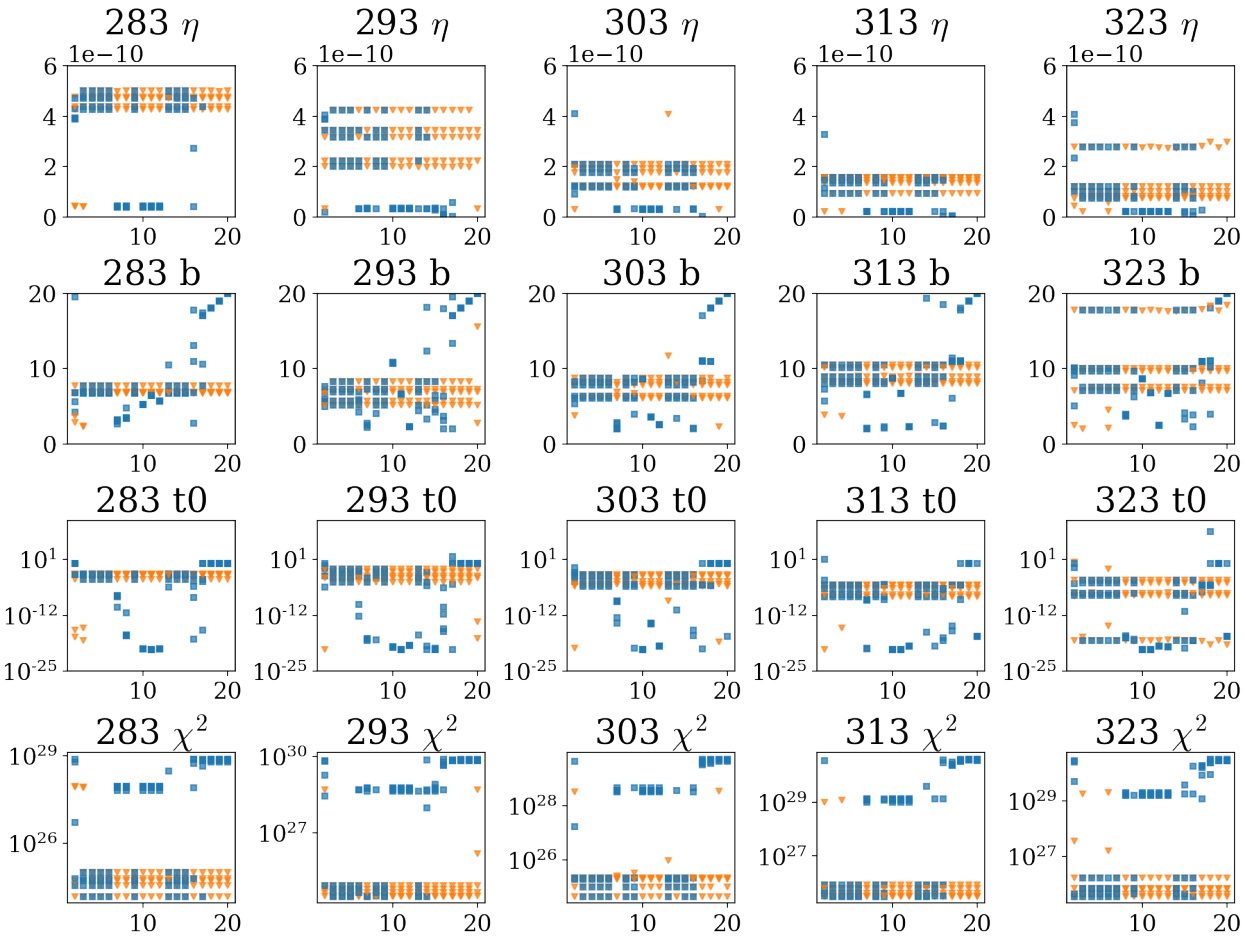

Figure S6: In each of these plots, the x-axis is the initial assumed value for b in the fits. Each datapoint on a single plot is the result of an individual fit. Results from all five replicas are shown on each plot. Orange triangles are results from basin-hopping fits, and blue squares are results from least-squares fits.

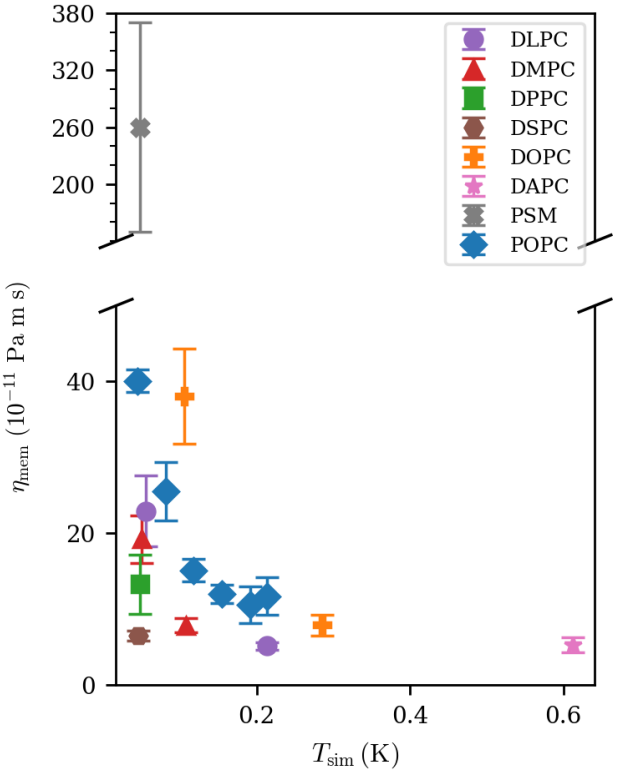

Figure S7: The viscosities of all systems studied in the present work, plotted against reduced temperature.

S 6 GENERATING RANDOM DATA WITH A STRETCHED-EXPONENTIAL AUTOCORRELATION FUNCTION

Let us define two functions, $r(t)$, which will be normally distributed white noise, and the goal autocorrelation function $C_g(t)$. Further defining:

$$\mathscr{F}\left[C_g(t)\right] = S(\omega) = \tilde{h}(\omega)^2 \tag{4}$$

where $\mathscr{F}[f]$ and $\tilde{f}$ both denote the Fourier transform of f. Then $C_g(t) = h(t) * h(t)$, where $*$ denotes convolution. Now define $x(t) \equiv r(t) * h(t)$. Computing $C_{xx}(t)$, the autocorrelation function of x, via its Fourier transform, we find

$$\tilde{C}_{xx}(\omega) = \mathscr{F}[x(t) * x(t)] = \tilde{x}(\omega)^2 = \left(\tilde{r}(\omega)\tilde{h}(\omega)\right)^2 = \tilde{r}(\omega)^2\tilde{h}(\omega)^2 \tag{5}$$

$$C_{xx}(t) = [r(t) * r(t)] * [h(t) * h(t)] = \delta(t) * C_g(t) = C_g(t) \tag{6}$$

and thus this definition of $x(t)$ gives the desired autocorrelation function.

In practice, we take the discretized goal autocorrelation function $C_g(t)$ on $t \in [0, \mathtt{L} \cdot \mathtt{dt}]$, we compute its power spectrum:

$$S(\omega) = \left|\mathtt{fft}\left[C_g(t)\right]\right| \tag{7}$$

specifically, we use the 'Hermitian fast fourier transform' algorithm, which assumes that $C_g^\star(-t) = C_g(t)$ ($f^\star$ denoting the complex conjugate of f) which holds, as $C_g(t)$ is real and symmetric. This effectively doubles the number of datapoints going into a regular Fourier transform—if $C_g(t)$ is L datapoints in length, then $S(\omega)$ has a length of $2L - 2$. Then $h(t) = \mathtt{fft}^{-1}[\sqrt{S(\omega)}]$.

We then generated a normally distributed signal $r(t)$. At this point we have everything needed to generate a signal $x(t)$ with autocorrelation of $C_g(t)$, via

$$x_i = \sum_{j=0}^{L} r_j h_{|i-j|} = \sum_{j=0}^{i} r_j h_{i-j} + \sum_{j=1}^{L} r_j h_{j-i}. \tag{8}$$

As a note, a time series generated using this method is non-Markovian; a given x_i depends on all $r_{j\leq i}$ *as well as* all $r_{j>i}$.

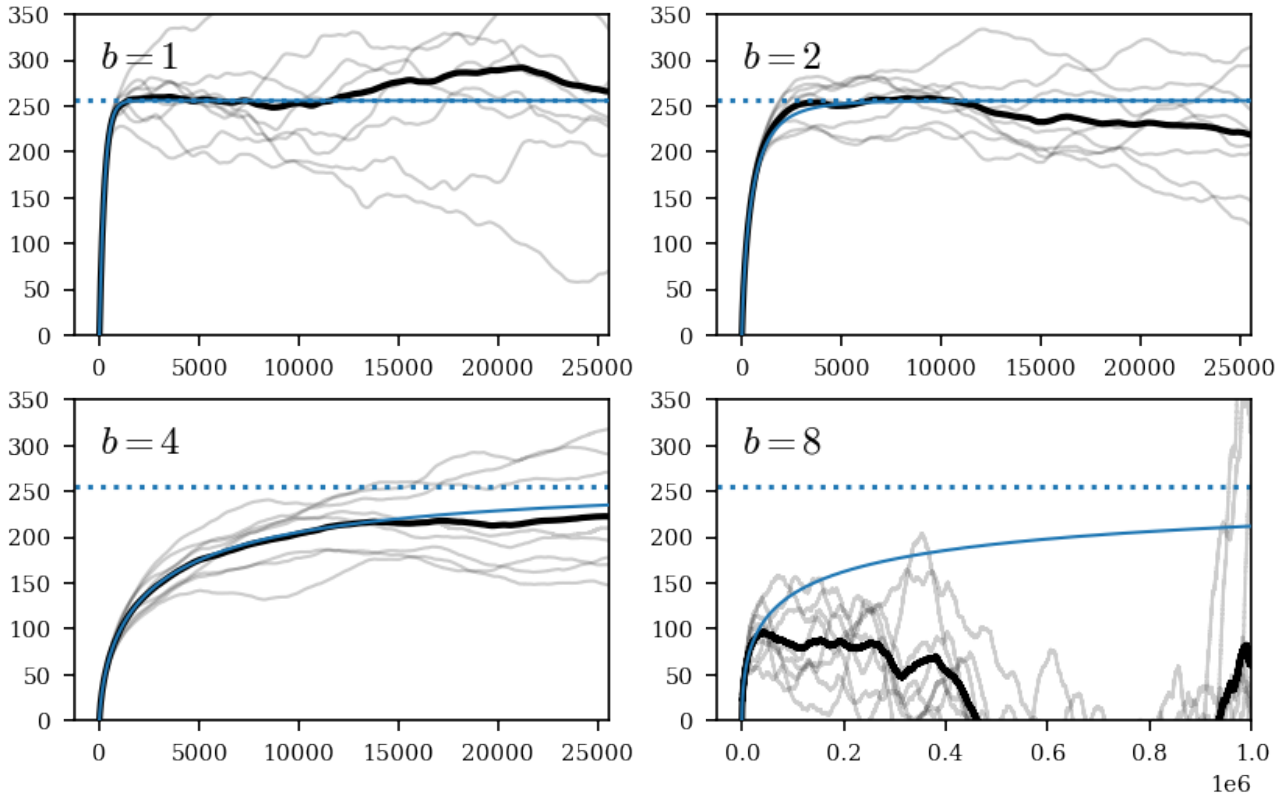

Figure S8: Numerically generated timeseries which follow a stretched exponential decay. 8 datasets of each were generated (light gray lines), with a full trajectory length of 1M timesteps. The average of the 8 samples is shown in black, and the 'true' autocorrelation function is in blue, with its asymptote as a blue dotted line. Note that the first three plots ($b = 1, 2, 4$) show 100× the mean relaxation time $\langle\tau\rangle$, while the final plot shows the entire signal, (nearly 4000× the mean relaxation time).

SUPPORTING REFERENCES

1. Berendsen, H. J., J. P. Postma, W. F. V. Gunsteren, A. Dinola, and J. R. Haak, 1998. Molecular dynamics with coupling to an external bath. *The Journal of Chemical Physics* 81:3684.

2. Mao, Y., and Y. Zhang, 2012. Prediction of the Temperature-Dependent Thermal Conductivity and Shear Viscosity for Rigid Water Models. *Journal of Nanotechnology in Engineering and Medicine* 3.

3. Fulcher, G. S., 1925. Analysis of Recent Measurements of the Viscosity of Glasses. *Journal of the American Ceramic Society* 8:339–355.

4. Wales, D. J., and J. P. K. Doye, 1997. Global Optimization by Basin-Hopping and the Lowest Energy Structures of Lennard-Jones Clusters Containing up to 110 Atoms. *The Journal of Physical Chemistry A* 101:5111–5116.